Agronomy Research **20**(S1), 1072–1089, 2022
https://doi.org/10.15159/AR.22.010

Geogenic and anthropogenic contamination of groundwater in a fragile eco-friendly region of southern Kerala, India

G. Prasad[1,*], H. Mamane[2] and M.V. Ramesh[3]

[1]Department of Mechanical Engineering, Amrita Vishwa Vidyapeetham, Amritapuri, India
[2]School of Mechanical Engineering, Faculty of Engineering, Tel Aviv University, Tel Aviv 69978, Israel
[3]Center for Wireless Networks and Applications (WNA), Amrita Vishwa Vidyapeetham, Amritapuri, India
[*]Correspondence: geena@am.amrita.edu

Received: January 25th, 2022; Accepted: March 1st, 2022; Published: March 17th, 2022

Abstract. In environmentally fragile regions that rely solely on groundwater resources, the hazards to the environment and human health are amplified by geogenic and anthropogenic pollution through the supply and use of groundwater for drinking and irrigation use. Groundwater from borewells in the study area was evaluated through hydrogeochemical analysis of 17 parameters in 2018 and 2019 across three seasons: pre-monsoon, monsoon, and post-monsoon. The study area, Kainakary, a fragile eco-friendly area in South India, was specifically chosen, as agriculture is the predominant anthropogenic activity in the region and other anthropogenic activities with known negative effects are negligible compared to other parts of India. Despite diligent attention paid to sustainable practices in Kainakary, iron, fluoride, and ammonia components in groundwater exceeded the permissible limits stipulated by the World Health Organization and Indian drinking water standards. Significant need for water resources due to below sea level farming practices of rice cultivation and potable water requirements result in over-extraction of groundwater, an inevitable cause of geogenic pollution. Anthropogenic pollution of groundwater sources was evidenced by the presence of coliform bacteria in samples. Determining the origins of major geogenic and anthropogenic pollutants, as well as understanding irrigation use patterns, play a key role in mitigating the overuse of groundwater sources. This study contributes to evolving strategies for reducing geogenic and anthropogenic pollution and for groundwater management in ecologically fragile areas toward achieving Sustainable Development Goal 12, which focuses on responsible consumption and production.

Key words: fluoride, groundwater, geogenic pollution, Kainakary, SDG 12.

INTRODUCTION

Many countries worldwide are facing acute water scarcity, due to increasing demand for, and diminishing availability of this resource. Rapid depletion of groundwater resources has resulted in distress for nearly 30% of the world's largest groundwater systems. Unavailability of accurate knowledge of the quantity of groundwater sources and inadequate monitoring and quality of these sources are hampering the ability to make

informed decisions. Water pollution, population density, and economic growth is now viewed as a threat to sustainable development (Boretti & Rosa, 2019).

Groundwater is considered to be safer than surface water in terms of quality and mineral composition, and to a certain extent, to be beneficial for human health (Rohde et al., 2017). Therefore, most of the effort currently revolves around groundwater availability to fulfill the water demands of an increasing population, rather than its quality for drinking purposes. Groundwater quality is impacted by natural hydrochemical and geochemical processes, increased groundwater abstraction, and potential contaminants from agriculture, human excreta and sanitation, industry, mining, solid waste disposal, and landfill leachate. To safeguard groundwater quality and quantity, in 2006, the Ground Water Rule was implemented in the USA and the Groundwater Directive in Europe.

India is among the largest groundwater users (Chinnasamy & Agoramoorthy, 2015; Mukherjee et al., 2015; Kulkarni et al., 2015; Patel et al., 2016; Arun, 2017). As of April 2015, the water resource potential of India was 1,869 billion cubic meter (BCM) per year in terms of natural runoff (water flow) in rivers. However only ~60% of it was usable due to its erratic and variable distribution and topographical constraints. The usable 1,123 BCM per year is comprised of 690 BCM per year of surface water and 433 BCM per year of groundwater (Central Water Commission, 2015). A report by NITI Aayog, the Indian government's think tank, has forecasted that by 2030, India's water demand will be twice the available supply, resulting in nearly 6% loss in GDP (NITI Aayog, 2018).

Hard-rock aquifers with poor permeability to recharge through rainfall are a predominant characteristic of nearly 65% of peninsular India. Over extraction of groundwater results in deterioration of groundwater quality (Mukherjee et al., 2015). Discharge from industrial waste, agricultural activities, urban wastewater, seawater intrusion in the coastal tract, and landfill leachate are common groundwater contaminants (Banerjee et al., 2012). Harmful substances in the groundwater in many parts of India are directly related to anthropogenic factors, specifically agricultural water use and landscape changes (Burow et al., 2017; Verma et al., 2017; Jia et al., 2018; Prasad et al., 2020). Fluoride and arsenic are the major geogenic contaminants of groundwater in India, and a major health concern, stemming from weathering processes (Banerjee et al., 2012). Increased incidence of chronic kidney disease associated with uranium has also been reported in India (Rajapurkar et al., 2012). Fluorosis associated with fluoride intake is common in Rajasthan (Agrawal et al., 1997; Choubisa, 2001).

According to a 2011 Indian census, groundwater through dug wells and borewells/tube wells is the source of potable water for nearly 65% of the population in the State of Kerala (Nair et al., 2014). Over the last 100 years, the per capita water availability in Kerala has decreased dramatically, while water demand has markedly increased. Kerala receives 2.5 times more rainfall than the national average in India, but it supports an ~4-fold population than the national average, as well as water utilization by a rich and diverse vegetation (Varma, 2017). Groundwater in Kerala is vulnerable to both geogenic and anthropogenic pollution. The Critical Zone, which extends from the treetops to the aquifer bottom, has exhibited drastic changes as a result of environmental degradation, poor water management, and urbanization. Moreover, changes in groundwater quality are evident in the pre-monsoon (PrM), monsoon (Mon), and post-monsoon (PoM) seasons. Manjula & Warrier (2019) opined that the groundwater and river water chemistry in regional studies in Kerala is influenced by existing rock chemistry rather than by precipitation and evaporation. Hydrochemistry analyses

revealed that Na^+ with Ca^{2+}, Cl^- and K^+ are dominant during the PrM season, whereas Ca^{2+} and mg^{2+} are dominant during the Mon season and HCO_3^- during the PoM season, possibly resulting from hydrochemical reactions in the aquifer, as posited by Vutla & Ravichandran (2011). Reza & Singh (2019) found a higher concentration of dissolved metals during the PrM vs. PoM season, probably due to more dissolution of metals during rock–water interactions in the relatively stagnant and low groundwater flow in the former season. Jasmin & Mallikarjuna (2014) showed that concentrations of eight parameters (total dissolved solids [TDS], nitrate [NO_3^-], N, Na^+, Cl^-, K^+, F^- and hardness) exceed their permissible limits during PrM and PoM seasons, with quality in the latter being worse than in the former season in the state of Tamil Nadu in Southern India, probably due to increased influx of contaminants from industries, mining areas, waste-disposal sites and agricultural fields during the monsoon season. Taken together, there is a pressing need for a better understanding of the quality of groundwater sources, its changing pattern before, during, and after monsoons, and the related anthropogenic factors, to ensure the sustainability of water resources and sustainable agriculture.

This study was carried out in a region where agriculture is the major anthropogenic activity, whereas other potentially negative anthropogenic activities are minimal. The goal of this study was to (i) compare groundwater quality parameters before, during, and after the monsoons, (ii) determine the presence of geogenic and anthropogenic pollution and identify the predominant pollutants (iii), determine the Water Quality Index (WQI) of groundwater sources for 2018 and 2019 in Kainakary, Kerala, and provide suitable management strategies for the region. The insights gained from this study will aid policymakers to implement appropriate management strategies for managing geogenic and anthropogenic pollution towards achieving sustainable development.

MATERIALS AND METHODS

Assessment of the geogenic and anthropogenic contaminants and the extent of pollution was done using previous and current analytical data, aggregated observations, and historical government data, due to the limited accessibility to region-specific data on the availability, water quality, and recharge practices.

Study Area

Alappuzha, the smallest coastal district in southern Kerala, is situated between latitudes 9°51' N and 9°45' N, and longitudes 76°45' E and 76°1' E (Prasad & Ramesh, 2019). The study area, Kainakary Panchayat (aka Grama Panchayat - village council in India), is an ecologically sensitive area of the Kuttanad wetland ecosystem and is an important tourist destination in India, attracting millions of people from within and outside the country. Apart from tourism, the study area is globally recognized as a Ramsar site- a wetland site listed under UNESCO's Ramsar Convention to promote sustainable use of its natural resources. The mission of the Ramsar Convention is 'the conservation and wise use of all wetlands through local and national actions and international cooperation, as a contribution towards achieving sustainable development throughout the world' (Gardner & Davidson, 2011). According to a 2011 Indian census (Census, 2011), the estimated population of Kainakary was 23,696 residents in 5,689 households. The practice of paddy field farming below sea level is a distinctive feature of agriculture in this area. Battered by heavy rainfall, the area is prone to severe floods,

disrupting the ecosystem's natural balance with devastating environmental consequences, as evidenced by the flooding havoc in 2018. The study area is a peninsula, and the landmass is interspersed with canals, ponds, and paddy fields.

Warkalli beds of Tertiary Age (Upper Miocene to Pliocene), the dominant geological feature of this region, are comprised of alternating beds of clayey sandstone, white and variegated clay, and carbonaceous clay. Notable lithological features in the study area include ferruginous laterite at depths of 0–6 m and 36–61 m. Data from government sources indicate that the phreatic aquifer is polluted in the study area. The geographical features, such as annual rainfall, temperature, geology, geomorphology, land-use pattern, soil, and detailed specifications of the study area have been elaborated by Prasad & Ramesh (2019).

Sampling

Three borewells, located at the outskirts of Kainakary Panchayat (approximately 6.5 km away from Alappuzha's town center), are the sole source of potable water for the entire population. Samples were collected during three seasons of the year in 2018–2019 from Kainakary Panchayat: (i) pre-monsoon (PrM), from February to May, (ii) monsoon (Mon), from June to September, and (iii) post-monsoon (PoM), from October to January. The sample nomenclature and locations are listed in Table 1. The collection of water samples conformed to APHA standard methods (Baird, 2017), and analyses were performed within 48 h of collection.

Table 1. Sample nomenclature and location

Sample name	Source	Depth	Location coordinates
S1	Borewell	120 m	9°47'17.4"N, 76°36'21.7"E
S2	Borewell	108 m	9°46'34.1"N, 76°36'44.6"E
S3	Borewell	80 m	9°46'52.1"N, 76°36'40.6"E

Analytical methods

The water samples collected were analyzed in the laboratory for physical, chemical, and biological parameters employing the standard methods (American Public Health Association; Baird 2017). Sample pH was measured using a portable pH meter (Eutech PCS Testr 35), color, turbidity, and hardness were determined by a Systronics Digital Nephelo Turbidity Meter, which was set to 100 with 40 NTU standards, electrical conductivity (EC) was measured by a portable conductivity meter (Elico) and TDS was computed by the EC meter. Analyses of the physicochemical and bacteriological parameters followed standard methods (Baird, 2017). A flame photometer (Systronics India Ltd.) was used to estimate the Na^+ and K^+ contents in the water. To estimate total hardness (TH) and calcium Ca^{2+} contents, the EDTA titrimetric method was used, whereas mg^{2+} levels were computed. Total alkalinity (TA) and bicarbonate (HCO_3^-) were determined by acid titration, and sulfide (S^{2-}) and Cl^- were determined by argentometric titration. A UV–VIS spectrometer (Thermo Scientific Evolution 201) was used to quantify Fe, sulfate (SO_4^{2-}), NO_3^-N, total ammoniacal nitrogen (TAN), and F^- levels. Phenolic compounds were estimated by spectrophotometry. Total coliform and Escherichia coli were determined by the most probable number (MPN) method. A Piper trilinear diagram (Piper, 1944), illustrating the predominant hydrochemical facies, was plotted with Aquachem Scientific software version 4.0 (AqQA).

RESULTS

Physicochemical Parameters

Physicochemical characteristics can provide insights into the nature of contaminants present in the groundwater sources of Kainakary Panchayat during the PrM, Mon, and PoM seasons. The range, average, and standard deviation of the measured physicochemical parameters of these samples obtained during 2018 and 2019 are summarized in Table 2.

Color of the samples ranged from 1–9 Hazen units (HU). In 2018, more than 50% of the PrM samples exhibited color above the acceptable limit of 5 HU (WHO, 2011); overall these samples showed more color in both years. Turbidity was above acceptable limits in the PrM samples from both years and the PoM samples. The pH of the groundwater samples in the study area varied from 6.90 to 8.00, indicating a slightly alkaline nature and conforming to World Health Organization (WHO) standards and Bureau of Indian Standards (BIS). EC is a good indicator of groundwater water quality, as groundwater will have more dissolved ions than surface water (RamyaPriya & Elango, 2018). The EC values of the samples ranged from 460 to 1,381 µS cm^{-1}. The estimated TDS values calculated from the EC values varied between 290 and 870 mg L^{-1}. According to the WHO (2011), TDS level in potable water should be less than 500 mg L^{-1}. Apart from S2 (for all seasons) in 2019, TDS values for all samples exceeded permissible limits, indicating that these sources are less suitable as drinking water and require treatment to meet potability standards. Cl^-, a major inorganic anion in groundwater, ranged between 56.4 and 280 mg L^{-1} in 2018 and 2019. Cl^- levels in the S1- PrM and S1- Mon samples were above the WHO limit. Fig. 1 shows the average Fe concentration in PrM, Mon, and PoM borewell samples. The limit specified by the WHO and BIS for Fe is 0.3 mg L^{-1}. In 2018 (except for one value in the Mon season), all samples showed high Fe concentrations; in 2019, all Mon values showed a decrease in concentration compared to the preceding year (Fig. 1).

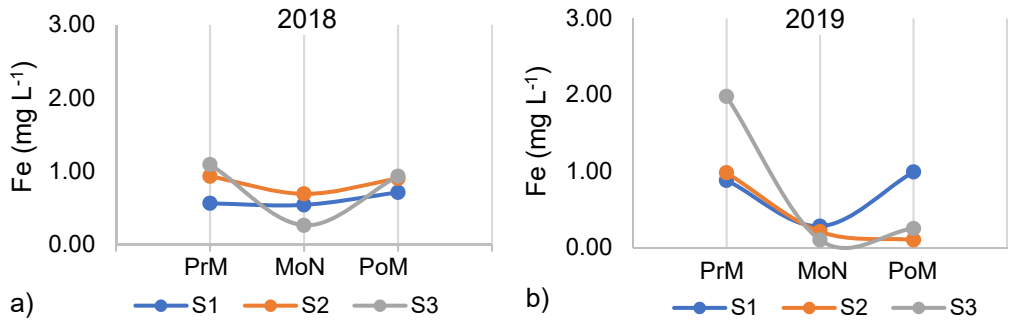

Figure 1. Fe concentration in borewell samples in 2018 (a) and 2019 (b).

Fig. 2 shows the average F concentrations in the PrM, Mon, and PoM groundwater samples. F^- levels in the samples from the study area were between 0.75 and 1.8 mg L^{-1}. The acceptable and permissible limits for F^- in groundwater are 1.0 mg L^{-1} and 1.5 mg L^{-1}, respectively (BIS, 2012). F^- was above safe limits in all borewells in the Mon seasons of both years.

Table 2. Physicochemical analyses and corresponding drinking water standards of the World Health Organization (WHO, 2011) and Bureau of Indian Standards (BIS, 2012)

Parameter	2018			2019			WHO 2011	BIS 2012	
	PrM	Mon	PoM	PrM	Mon	PoM		AL	PL
Color (HU)	5–9 (7.0 ± 2.0)	2–4 (3.0 ± 1.0)	5–6 (5.33 ± 0.58)	2–4 (3.0 ± 1.0)	1–1 (1 ± 0)	1–2 (1.3 ± 0.6)	5	5	15
Turbidity	2.2– 4.3 (2.97 ± 1.16)	0.8–1.8 (1.3 ± 0.5)	1.5–2.1 (1.83 ± 0.31)	2.1–2.3 (2.17 ± 0.12)	0.4–1.0 (0.7 ± 0.30)	1.0–2.8 (1.67 ± 0.99)	1.5	1	5
pH	6.90–7.20 (7.05 ± 0.15)	6.75–7.11 (6.92 ± 0.18)	7.20–7.43 (7.28 ± 0.13)	6.93–8.00 (7.3 ± 0.61)	6.98–7.16 (7.05 ± 0.1)	7.30–7.43 (7.36 ± 0.07)	6.5–8.5	6.5–8.5	NR
EC (µS cm^{-1})	463–1249 (749, ± 434.88)	460–998 (687 ± 303.06)	619–1380 (947, ± 391.82)	655–1278 (920, ± 321.62)	655–1373 (962 ± 367.30)	703–1281 (949 ± 298.05)	1,500	–	–
TDS (mg L^{-1})	336–787 (471.67 ± 273.97)	290–629 (433 ± 175.6)	390–870 (596.67 ± 246.85)	413–805 (579.33 ± 202.62)	419–865 (606.33 ± 231.4)	443–807 (598.33 ± 187.77)	500	500	2,000
Na^+ (mg L^{-1})	22.30– 142.10 (67.5 ± 65.09)	24.50–84.70 (53.83 ± 30.13)	28.20–92.80 (60.2 ± 32.3)	26.80–108.20 (61.23 ± 42.12)	39.40–113.80 (72.43 ± 37.89)	31.40–82.80 (58.53 ± 25.82)	200	–	–
K^+ (mg L^{-1})	0.7–1.2 (0.97 ± 0.25)	1.0–3.4 (2.1 ± 1.21)	0.9–2.6 (1.63 ± 0.87)	0.5–0.9 (0.67 ± 0.21)	0.8–2.2 (1.37 ± 0.74)	0.7–1.9 (1.17 ± 0.64)	12	–	–
TH (mg L^{-1})	78.3–186.2 (117.73 ± 59.52)	85.6–168.6 (121.03 ± 42.81)	104.0–220.0 (155.37 ± 59.13)	87.1–198.0 (125.75 ± 62.62)	112.0–220 (158.87 ± 55.4)	116–200 (155.33 ± 42.25)	–	200	600
Ca^{2+} (mg L^{-1})	19.6–53.6 (31.5 ± 19.16)	19.7–43.9 (29.47 ± 12.76)	27.2–50.16 (36.25 ± 12.23)	19.17–46.1 (29.16 ± 14.75)	28–44.1 (34.9 ± 8.29)	28.0–38.0 (32 ± 5.29)	75	75	200
Mg^{2+} (mg L^{-1})	7.52–21.8 (12.8 ± 7.34)	10.2–17.36 (13.72 ± 3.58)	12.89–24.88 (18.56 ± 6.02)	9.2–20.2 (13.73 ± 5.75)	12.1–23.7 (17.72 ± 5.81)	14.0–27.0 (18.67 ± 7.23)	50	30	100
Cl^- (mg L^{-1})	56.8–280.0 (141.8 ± 120.74)	57.4–245.8 (135.73 ± 98.13)	60–190 (120.67 ± 65.43)	56.4–270.8 (144.33 ± 112.27)	83.4–156.8 (172.73 ± 98.27)	68.0–219.0 (138.33 ± 76.03)	250	250	1,000
TA (mg L^{-1})	148.36–208.20 (157.41 ± 46.92)	131.15–155.74 (144.75 ± 12.5)	163.28–205.74 (179.68 ± 22.82)	113.90–179.51 (148.27 ± 32.91)	152.61–207.38 (182.23 ± 27.66)	170.49–195.00 (180.31 ± 13.02)	500	200	600
Fe^{2+} (mg L^{-1})	0.56–1.09 (0.86 ± 0.27)	0.26–0.69 (0.5 ± 0.22)	0.71–0.93 (0.85 ± 0.12)	0.88–1.98 (1.28 ± 0.61)	0.1–0.28 (0.2 ± 0.09)	0.1–0.99 (0.45 ± 0.48)	0.3	0.3	NR
SO_4^- (mg L^{-1})	3–5.2 (4.20 ± 1.11)	1.02–2 (1.37 ± 0.54)	2.28–4.2 (2.98 ± 1.06)	3.32–5.03 (3.90 ± 0.98)	2.22–4.07 (3.13 ± 0.93)	4.96–6 (5.39 ± 0.54)	250	200	400
NO_3-N (mg L^{-1})	1.06–1.45 (1.21 ± 0.21)	1.72–3.77 (2.49 ± 1.11)	3.72–5.91 (4.93 ± 1.11)	1.6–2.70 (2.32 ± 0.62)	1.25–3.30 (1.98 ± 1.14)	2.89–4.40 (3.83 ± 0.82)	45	45	NR
F^- (mg L^{-1})	1.02–1.13 (1.07 ± 0.06)	1.08–1.46 (1.32 ± 0.21)	0.98–1.8 (1.5 ± 0.45)	0.75–1.43 (1.08 ± 0.34)	0.98–1.22 (1.12 ± 0.12)	0.89–1.49 (1.29 ± 0.34)	–	1	1.5
TAN (mg L^{-1})	3.82–4.51 (4.51 ± 0.7)	3.18–4.1 (3.59 ± 0.47)	3.34–4.85 (4.23 ± 0.79)	3.04–5.6 (3.94 ± 1.44)	6.69–8.96 (7.15 ± 1.63)	3.98–5.96 (4.72 ± 1.08)		0.5	NR

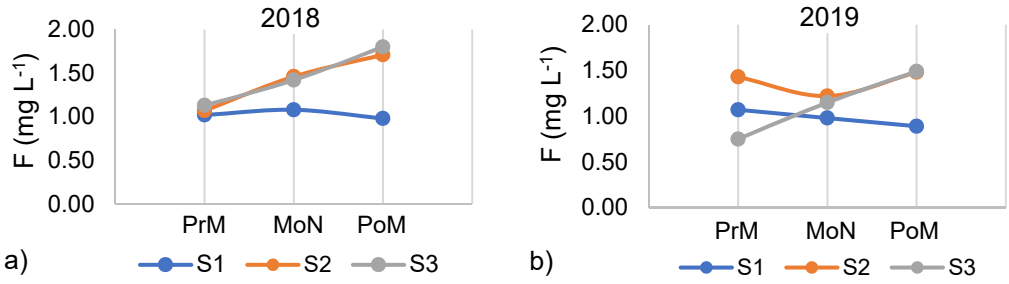

Figure 2. F concentration (mg L^{-1}) in borewell samples in 2018 (a) and 2019 (b).

TAN is the total amount of nitrogen as ammonia (NH_3) and dissolved ammonium ions (NH_4^+). Fig. 3 shows the average TAN concentrations in the borewell samples for the PrM, Mon, and PoM seasons. Total NH_3 was much above the permissible level of 0.5 mg L^{-1} in all groundwater sources in all seasons.

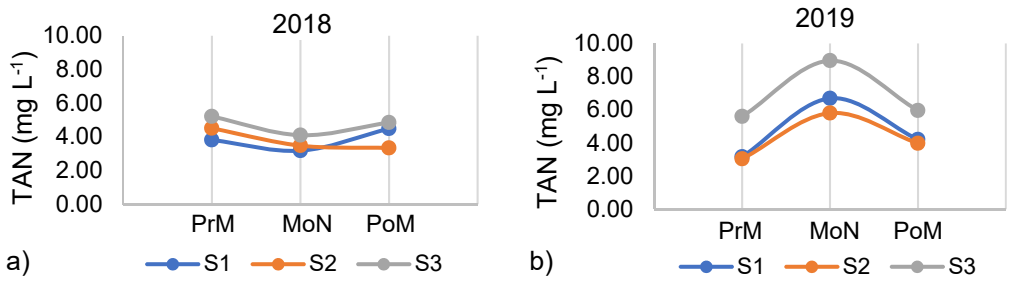

Figure 3. TAN level (mg L^{-1}) in borewell samples in 2018 (a) and 2019 (b).

TA, SO_4^{2-} and NO_3^- were found to be within the permissible limits in all samples across all seasons. Values of Al, phenolic compounds, and S^{2-} in the water samples were below detection limits across all seasons in 2018 and 2019.

DISCUSSION

The color of the samples is possibly due to reduced groundwater volumes during the PrM season. Turbidity in groundwater is caused mainly by clay, silt, reduced Fe precipitates, and other oxides originated from the erosion of rocks in aquifers, vegetative debris, and microorganisms present in water bodies (Baluch & Hashmi, 2019; Cheremisinoff, 2019). We have done a survey in the study area and the participants indicated that the water supply through faucets was visibly muddy quite often. The particulate matter responsible for turbidity settles at the bottom of the storage tanks, making the water dirtier, even during the supply of clear water, and coalescing of particulate matter can potentially clog water piping (Cheremisinoff, 2019), which is commonly seen in the study area. High turbidity in potable water can be associated with a higher incidence of infections of the human gastrointestinal tract (WHO, 2011).

Significantly increased rainfall, a departure from normal rainfall pattern, during the months of July and August in both the years (IMD Annual Report 2018 and IMD Annual

Report 2019), did significantly influence the pH of groundwater. Bicarbonates, originating from carbonate minerals and dissolved soil gases, are the major contributors to the natural alkalinity of groundwater. Point source pollution from rainwater and floodwater runoff, wastewater discharge, or anthropogenic activities also contribute to the alkalinity of surface water (Mattson, 2009; Prasad et al., 2021).

Higher values of EC can reduce the aesthetic appearance of water and are also insensitive to infants and heart patients (WHO, 2003). Variations in TDS are probably a result of geogenic pollution, such as weathering of sedimentary rocks and erosion of the earth's surface resulting in the formation of salts as NaCl, Ca^{2+}, Mg^{2+} and K^{+}, SO_4^{-}, and HCO_3. These salts can accumulate through the continuous process of precipitation and evaporation. Higher levels of TDS in groundwater are usually a result of its contact time with underlying rocks and sediments (Gjessing, 1976). Excessive solids impart an undesirable taste, emanating primarily as Cl^{-} content in the water, as well as gastrointestinal irritation.

Chloride in groundwater is contributed by both natural and anthropogenic sources, as runoff containing fertilizers, landfill leachates, industrial and sewage effluents, irrigation drainage, and seawater intrusion in coastal areas (WHO, 2003). Cl^{-} as an anthropogenic pollutant can be attributed to agricultural activities, particularly paddy cultivation as frequent washing of the soil with burnt lime is undertaken to neutralize alkalinity (FAO, 2016). The presence of Cl^{-} rich minerals or rocks are the sources of geogenic contamination. Cl^{-} exists as NaCl in groundwater; however, the Cl^{-} content may exceed that of Na due to the phenomenon of base exchange. CaCl and MgCl are rare in groundwater (Nair et al., 2018).

Fe is present naturally in soils, rocks, and minerals, and is a constituent in oxides, hydroxides, sulfides, sulfates, arsenates, and carbonates. Fe can be present in groundwater due to weathering of Fe-bearing minerals in rocks. When the concentration of Fe approaches 0.3 mg L^{-1}, the water has a metallic taste and becomes less potable. Natural mobilization of Fe from alluvial deposition and natural recycling are the sources of Fe in the Alappuzha region, in which the study area belongs. Increased mobilization of Fe is seen when the increased speed of water flow occurs, especially during monsoon season and flooding instances (Sivanandan & Ambili, 2018), which is not a rare incident in this region. Groundwater that is acidic or low in oxygen may have higher dissolved Fe concentrations (Zucker et al., 2015). Increased well water volumes during the Mon season probably resulted in lower Fe concentration. Another peculiarity of this region is its effluent seepage from septic tanks, silage clamps from paddy fields, slurry pits, landfills, or other sources of anthropogenic pollution which can contribute Fe to the groundwater over long periods of time. Anaerobic groundwater can contain increased levels of Fe^{2+} without displaying any discoloration or turbidity when pumped directly from the well. However, oxidation of this Fe^{2+} to Fe^{3+} occurs upon exposure to the atmosphere, turning the water a reddish-brown color. Fe can also increase the growth of unwanted bacteria, resulting in biofouling in the well, pump, and water pipes (Bachmann & Edyvean, 2005). From the personnel communication, several villagers complained that in some parts of the study area they feel stringent odor in water. They often get muddy or reddish-brown colored water, which causes stains in the clothes, while washing. Fe deposits and biofouling can clog the intake of a well or affect the pump, making the well less efficient. At levels above 0.3 mg L^{-1}, Fe stains laundry and plumbing fixtures. Fe values of samples showed an increasing trend in the PrM period (Fig. 1).

F is a naturally occurring time-variant geogenic pollutant that is commonly found in bedrock as F minerals, such as F^-, hornblende, biotite, and fluorapatite (Nair et al., 2018). Managing F^- pollution is tricky because the source of the pollution is unknown. The tertiary sediments at Alappuzha- where the study area locates - shows the presence of a common mineral, fluorapatite, which is the source of fluoride in groundwater. The key factors accountable for the high fluoride content in the groundwater are sediment–groundwater interaction, prolonged residence time, and facies changes (Ca-HCO_3 to Na-HCO3) (Raj & Shaji., 2016). F^- is essential for healthy bones and teeth, and consumption levels below 0.5 ppm can lead to dental caries and weak bones in children (WHO, 2011). On the other hand, consumption of F^- in excess of 1.0 ppm can result in fluorosis of the bones and/or teeth (Susheela, 1991).

Intense agricultural activities during the monsoon season of 2019 resulted in a dramatic increase in TAN levels. The N cycle signifies the exchange and movement of N between plants, animals, the atmosphere, soil, microorganisms, surface water, and groundwater. N is found in nature as NH_3 as a result of the decomposition processes of organic material (Mahler & Garner, 2009; Prasad et al., 2020). Fertilizers, such as ammonium nitrate, manure used in agriculture in the study area, and occasionally, sewage contamination, are common reasons for anthropogenic pollution by NO_3^- and NH_3 (Zhang et al., 2018). NO_3^- is considered a reliable indicator of contamination resulting from agricultural activity. The causes for such high TAN levels in groundwater sources in Kainakary is a research focus for future work.

Hydrogeochemical Facies

The Piper (1944) trilinear diagram can be used to elucidate, compare and contrast the characteristics of groundwater (Todd, 1980). Plots of cations and anions and their concentrations using Aquachem Scientific software version 4.0 are shown in Fig. 4. The common water types in the study area were $CaHCO_3$ type, NaCl type, and mixed CaMgCl type. The predominance of Cl and HCO_3 types indicates sample salinity.

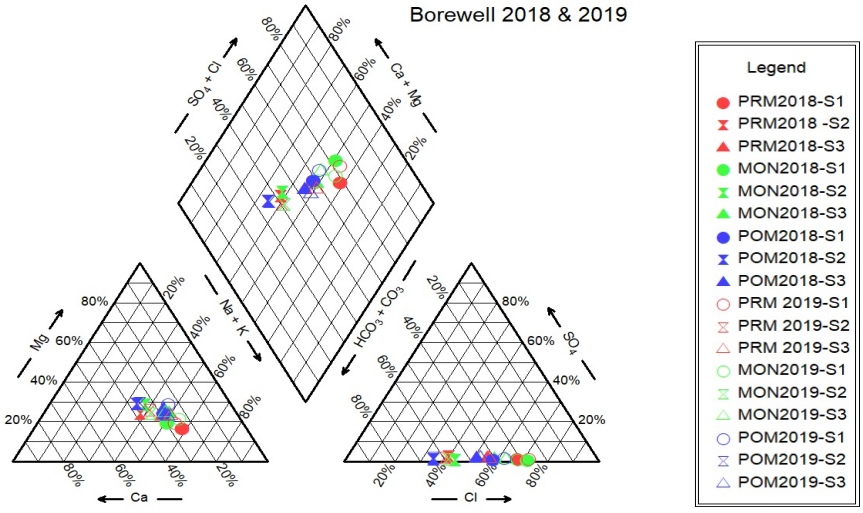

Figure 4. Piper diagram illustrating the relationship between dissolved ions in groundwater samples in PrM, Mon, and PoM seasons for 2018 and 2019.

Ionic Ratios

Ionic ratios of groundwater samples taken during the PrM, Mon, and PoM seasons for 2018 and 2019 are shown in Table 3, Fig. 5, and Fig. 6. The mean Ca^{2+}+ + Mg^{2+}/ Na^{+}+ K^{+} ratios during PrM, Mon, and PoM for each year (Table 3) indicated that the presence of Ca^{2+} and Mg^{2+} ions was due to silicate minerals (Katz et al., 1997; Nair et al., 2018). The mean HCO_3^-/ Ca^{2+} + Mg^{2+} ratios for the three seasons in 2018 and 2019 (Table 3) reflected a higher value during the PrM season. Higher HCO_3^-/ Ca^{2+} ratios were noted in the PoM season, an indication of increased dissipation of atmospheric CO_2 during rainfall. Minor fluctuations of ionic components were seen across the 2018 and 2019 seasons, indicating the absence of any drastic compositional change.

Table 3. Ionic ratios of groundwater samples during PrM, Mon, and PoM seasons for 2018 and 2019

Ionic Ratio	2018								
	PrM			Mon			PoM		
	Avg	Min	Max	Avg	Min	Max	Avg	Min	Max
Ca^{2+} + mg^{2+}/Na^{+} + K^{+}	1.14	0.71	1.60	1.21	0.96	1.63	1.40	1.11	1.91
HCO_3^-/Ca^{2+} + mg^{2+}	1.65	1.15	2.27	1.46	1.05	1.97	1.38	1.10	1.72
HCO_3^-/Ca^{2+}	2.75	1.90	3.69	2.65	1.73	3.65	2.53	2.00	3.05
Ca^{2+}/Na^{+}	0.70	0.43	1.01	0.69	0.55	0.92	0.78	0.61	1.11
Mg^{2+}/Na^{+}	0.47	0.28	0.64	0.55	0.39	0.78	0.64	0.51	0.86
Ca^{2+}/Mg^{2+}	1.49	1.34	1.59	1.28	1.11	1.54	1.20	1.07	1.29
Ca^{2+}/ SO_4^{2-}	17.50	10.72	24.74	58.68	29.76	103.29	32.46	17.94	52.80
Mg^{2+}/Ca^{2+}	0.67	0.63	0.75	0.80	0.65	0.90	0.84	0.78	0.93
HCO_3^-/HCO_3^- + SO_4^{2-}	0.98	0.98	0.98	0.99	0.99	0.99	0.99	0.98	0.99
Ionic Ratio	2019								
	PrM			Mon			PoM		
	Avg	Min	Max	Avg	Min	Max	Avg	Min	Max
Ca^{2+} + mg^{2+}/Na^{+} + K^{+}	1.09	0.84	1.45	1.10	0.83	1.37	1.33	1.02	1.84
HCO_3^-/Ca^{2+} + mg^{2+}	1.53	1.11	2.16	1.45	1.22	1.90	1.45	1.16	1.68
HCO_3^-/Ca^{2+}	2.75	1.90	3.85	2.61	2.28	3.25	2.78	2.51	3.06
Ca^{2+} /Na^{+}	0.61	0.49	0.82	0.62	0.45	0.82	0.71	0.53	1.03
Mg^{2+} /Na^{+}	0.49	0.35	0.65	0.49	0.39	0.58	0.64	0.46	0.84
Ca^{2+} /Mg^{2+}	1.27	1.15	1.39	1.23	1.14	1.41	1.10	0.86	1.22
Ca^{2+} / SO_4^{2-}	17.25	13.86	22.00	27.88	19.22	34.14	14.20	13.55	15.20
Mg^{2+} /Ca^{2+}	0.79	0.72	0.87	0.82	0.71	0.88	0.93	0.82	1.16
HCO_3^- /HCO_3^- + SO_4^{2-}	0.98	0.98	0.98	0.99	0.98	0.99	0.98	0.97	0.98

Bivariate diagrams (mixing diagrams) of Ca^{2+}/ Na^{+} vs. Mg^{2+}/ Na^{+} and HCO_3^-/ Na^{+} vs. Ca^{2+}/ Na^{+} for all seasons and years are given in Fig. 5 and 6, respectively, indicating that the groundwater's geochemical character is due to weathering of aluminosilicate minerals and atmospheric dissolution (Gaillardet et al., 1999).

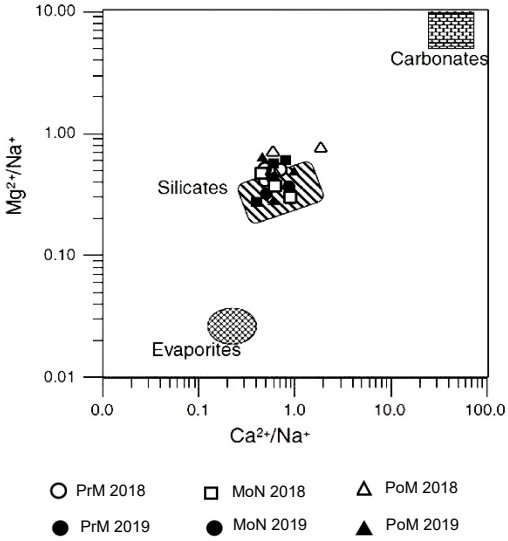

Figure 5. Scatter plot of mg^{2+}/Na^{+} vs. Ca^{2+}/Na^{+} relating carbonate and silicate members in the study area.

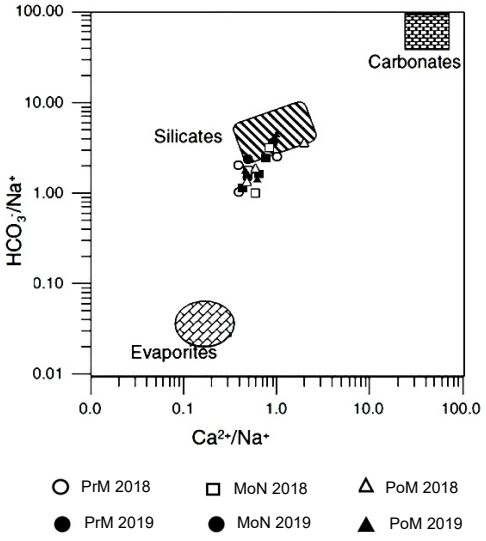

Figure 6. Scatter plot of HCO_3^{-}/ Na^{+} vs. Ca^{2+}/ Na^{+} relating carbonate and silicate members in the study area.

Ion Exchange

Ion-exchange processes can represent the variations in geochemical processes that lead to changes in potable water quality. The variation in the chemical composition of groundwater along its flow path is understood by studying the Chloro Alkaline Indices (CAI). Schoeller (1977) has recommended two Chloro-Alkaline Indices CAI-I and CAI-II for the interpretation of ion exchange between groundwater and the host environment. The Chloro-Alkaline Indices is expressed as:

$$CAI–I = Cl^{-} – (Na^{+}+ K^{+})/ Cl^{-}$$
$$CAI–II = Cl^{-} – (Na^{+}+ K^{+})/ (SO_4^{2-} + HCO_3^{-} + NO_3^{-}) \quad (1)$$

where, CAI–I and CAI–II are Chloro-Alkaline Indices.

The positive value of CAI in all samples indicates that the predominant base exchange is between Na^{+} and K^{+} ions in the water source and Ca^{2+} and mg^{2+} ions in the rocks, as shown in Table 4. It can be inferred that the water samples in this region are exposed to similar geochemical processes and the fate of the environmental contaminants is better predicted.

The tendency of Ca^{2+} and mg^{2+} to engage in reactions that leave insoluble mineral deposits rendering groundwater hard varies from region to region. Increasing hardness requires water treatment processes to be in place before delivery for potable and irrigation use. It is more difficult for plants to absorb and break down hard water when compared to soft water leading to an increased rate of irrigation to compensate for poor utilization. This in turn leads to additional strain on the groundwater resources.

Table 4. Total ion concentration and chloro-alkali index (CAI) of groundwater samples

Year	Season	Sample no.	TZ-	TZ+	CAI–I (meq L^{-1})	CAI–II (meq L^{-1})
2018	PrM	S1	13.16	14.35	0.33	1.18
		S2	5.42	4.16	0.39	0.2
		S3	5.46	5.31	0.33	0.35
	Mon	S1	10.89	10.76	0.39	0.73
		S2	5.51	4.65	0.34	0.17
		S3	6.29	6.83	0.29	0.33
	PoM	S1	10.69	13.05	0.24	0.3
		S2	6.53	5.76	0.27	0.11
		S3	7.59	8.49	0.24	0.22
2019	PrM	S1	12.31	12.65	0.38	0.74
		S2	5.47	4.64	0.26	0.13
		S3	6.02	6.05	0.29	0.34
	Mon	S1	13.19	13.55	0.37	0.62
		S2	7.05	6.37	0.27	0.15
		S3	8.31	8.75	0.37	0.49
	PoM	S1	11.26	11.76	0.38	0.49
		S2	6.60	6.26	0.31	0.13
		S3	8.19	8.42	0.34	0.29

TZ-, total anions; TZ+, total cations.

Coliform Counts

Studies have shown that nearly 70% of open wells in Kerala are rife with bacterial contamination (Harikumar & Chandran, 2013; Jaya Divakaran et al., 2019). Groundwater samples were analyzed to determine the presence of coliform bacteria, specifically E. coli, to assess source contamination due to anthropogenic activities. The presence of bacteria was confirmed in all borewells during the PrM and Mon seasons of 2018. PoM samples in 2018 were devoid of bacteria, which can be attributed to the extensive and elaborate chlorination measures following the great flood of August 2018. The presence of bacteria was noted in two of the three borewells during the Mon season of 2019, although at a lower concentration than in 2018, as shown in Fig. 7. One of the primary causes of water pollution is untreated wastewater, often discharged into streams, and affecting downstream water quality as well as lakes, open wells, and even deeper groundwater sources as seen during 2018 as a result of flooding (Jaya Divakaran et al., 2019; Amritanand et al., 2020), which is very familiar in the study area too.

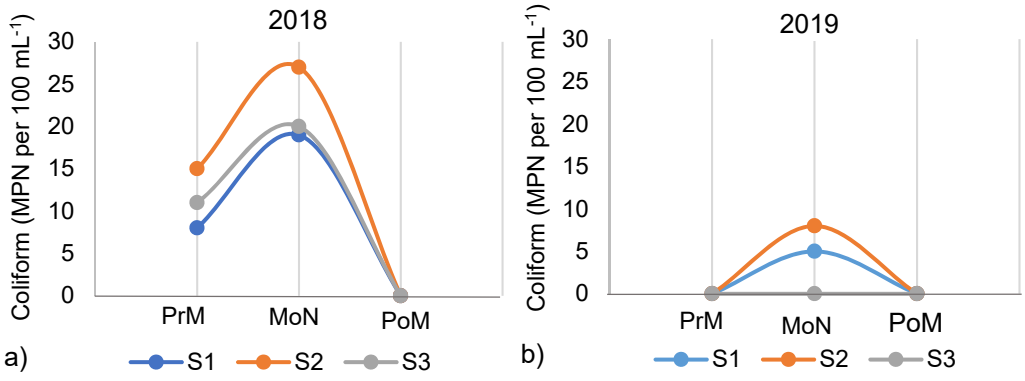

Figure 7. Bacteriological parameters of groundwater samples from the study area collected in the PrM, Mon, and PoM seasons of 2018 (a) and 2019 (b).

Drinking-Water Suitability

The WQI is the most common parameter for assessing the quality of drinking water. Various researchers have adopted different methodologies to calculate the WQI (Tiwari & Mishra, 1985; Mishra & Patel, 2003; Gebrehiwot et al., 2011; Nair et al., 2018). A WQI < 50 is indicative of excellent water quality and a WQI between 50 and 100 denotes good water quality. A WQI of 100–200 denotes poor water quality, and a WQI between 200 and 300 is indicative of very poor water quality. Finally, a WQI > 300 signifies a non-potable water source. The weightages (*wi*) accorded to the hydrochemical parameters on the basis of their impact on potable water quality and the computed relative weight (*Wi*) of the chemical parameter are highlighted in Table 5. Based on the concentration of the chemical parameters in the samples and the guideline values as defined by the BIS and the WHO, a quality rating scale was constructed.

Table 5. Weightage accorded to physicochemical parameters based on their impact on the quality of potable water (Gebrehiwot et al., 2011; Nair et al., 2018)

Chemical parameter	BIS (2012)	WHO (2011)	Weight (wi)	Relative weight (Wi)
pH	6.5–8.5	8.5	4	0.09
EC (µS cm^{-1})	500	500	4	0.09
TDS (mg L^{-1})	500	500	5	0.11
Na^{+} (mg L^{-1})	–	200	2	0.04
K^{+} (mg L^{-1})	–	12	2	0.04
TH (mg L^{-1})	200–600	–	3	0.06
Ca^{2+} (mg L^{-1})	75–200	75	2	0.04
Mg^{2+} (mg L^{-1})	30–100	50	2	0.04
TA (mg L^{-1})	–	500	3	0.06
Cl^{-} (mg L^{-1})	250–1,000	250	3	0.06
SO_4^{-} (mg L^{-1})	200–400	250	4	0.09
$NO_3^{-}N$ (mg L^{-1})	45	45	5	0.11
Fe^{2+} (mg L^{-1})	0.3	0.3	4	0.09
F^{-} (mg $L^{-1}L$)	1	1	4	0.09

Fig. 8 illustrates the decline in most of the WQI in the Mon and PoM seasons of 2018 and 2019. An improvement in the quality was noted in 2019, although it remained in the 'Good' category. The water must be treated to remove Fe, F^{-} and ammoniacal N components before its distribution through potable water systems.

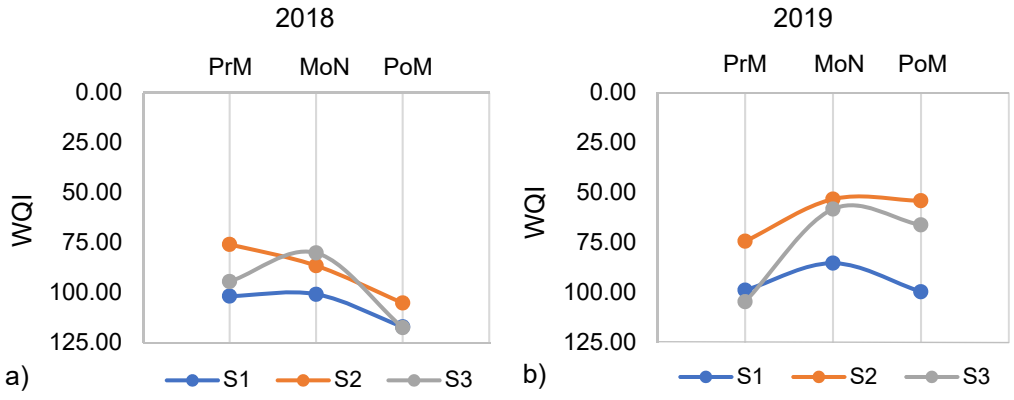

Figure 8. Water quality index of groundwater samples in the study area collected during the PrM, Mon, and PoM seasons of 2018 (a) and 2019 (b).

In August 2018, the state of Kerala witnessed a massive flood, which affected millions of people. The groundwater levels monitored by the Central Ground Water Board (CGWB) at the end of August 2018 in Kerala showed that the water level varied from less than 1 m to 20 m below ground level (Central Ground Water Board, 2020). A year-over-year comparison indicated a fall in water levels in most of the dug wells - 57.88% of the total wells monitored. There was a rise in water level in 41.45% of the wells, and only a few wells showed no change in water level, indicating that groundwater level did not increase considerably during Mon 2018. During periods of heavy rainfall, nearly 95% of rainwater ends up as surface runoff. However, in November 2018, 81% of the dug wells showed a rise in water level and only 19% showed a falling trend (CGWB, 2020), suggesting more groundwater recharge from the normal rainfall occurring in the PoM season than from the heavy spells, and this increased groundwater recharge resulted in improved groundwater quality.

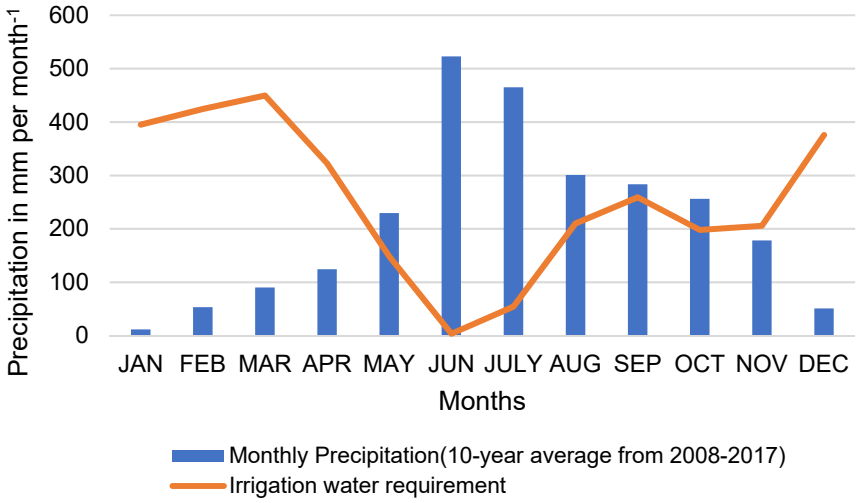

Figure 9. Ten year (2008–2017) average monthly rainfall vs monthly irrigation water need.

Understanding irrigation water requirements in the study area from the perspective of replenishment of water resources can promote both agriculture and sustainability. Fig. 9 illustrates the mismatch between the 10-year average (2008–2017) monthly irrigation needs versus the 10-year average monthly rainfall. Surplus rainfall during the monsoon season corresponds to minimal irrigation needs, while during the season of rice cultivation, the quantum of rainfall cannot minimize the extraction of groundwater to meet the irrigation water needs. Infrastructure to save surplus rainfall for groundwater recharge or to be utilized for conjunctive use in agriculture during non-rainy seasons can minimize the stress on groundwater resources in the study region.

CONCLUSIONS

Given that the region of study is an agricultural and eco-friendly zone, anthropogenic activities with deleterious effects were minimal relative to other regions in India. It is well known that point source pollution from wastewater and agricultural

runoff leads to polluted surface waters, however, the direct and indirect effects of surface water pollution on groundwater sources are yet to be elucidated. Anthropogenic contamination of the groundwater in the study area was evidenced by the presence of bacteria and NH_3 components and indicates interconnectivities between surface water and groundwater sources. Geogenic contamination of groundwater sources in the study region was evidenced by the presence of Fe and F- levels above permissible limits and are the result of natural geogenic processes exacerbated by over-extraction of groundwater for potable and irrigation use during dry seasons. Appropriate water treatment measures including defluoridation may be required to prevent health hazards. The observed improvement in water quality during PoM season was associated with groundwater recharge, reiterating that artificial recharge of groundwater could significantly remediate geogenic pollution and promote sustainable use of groundwater resources in the study region and other ecologically fragile areas. The need for responsible consumption of natural resources in the context of agriculture, the fabric of culture, and economic activity in Kainakary. contribute to the achievement of Sustainable Development Goal (SDG) 12 and other SDGs directly or indirectly, as they are all integrated. In addition, activities such as awareness campaigns, mitigation of flood risks and enforcement of rehabilitation measures, monitoring of groundwater quality periodically, and widening the observation areas, can supplement the natural replenishment of groundwater and reverse geogenic pollution, and achieve sustainable consumption and production patterns.

REFERENCES

Agrawal, V., Vaish, A.K. & Vaish, P. 1997. Groundwater quality: focus on fluoride and fluorosis in Rajasthan. *Current Science* **73**(9), 743–746.

Amritanand, S., Anand, S. & Amritesh, A.R., 2020, January. Dynamic and time critical emergency management for level three disaster: a case study analysis of Kerala floods 2018. In *Proceedings of the 21st international conference on distributed computing and networking* (pp. 1–6).

Arun, K. 2017. Geospatial approach for wind farm site selection-A Kerala scenario, 2017 *International Conference on Technological Advancements in Power and Energy* (TAP Energy), Kollam, pp.1–5.

Bachmann, R.T. & Edyvean, R.G.J. 2005. Biofouling: a historic and contemporary review of its causes, consequences and control in drinking water distribution systems. *Biofilms* **2**(3), 197.

Baird, R.B. 2017. Standard Methods for the Examination of Water and Wastewater, 23rd. Water Environment Federation, *American Public Health Association, American Water Works Association*.

Baluch, M.A. & Hashmi, H.N. 2019. Investigating the impact of anthropogenic and natural sources of pollution on quality of water in Upper Indus Basin (UIB) by using multivariate statistical analysis. *Journal of Chemistry*, **2019**

Banerjee, D.M., Mukherjee, A., Acharya, S.K., Chatterjee, D., Mahanta, C., Saha, D., ... & Raju, N.J. 2012. Contemporary groundwater pollution studies in India: a review. In Proc. *Indian Natl. Sci. Acad.* **78**(3), pp. 333–342.

BIS, I.S.D. W.S. 2012. Bureau of Indian Standards. New Delhi, 2–3.

Boretti, A. & Rosa, L. 2019. Reassessing the projections of the world water development report. *NPJ Clean Water* **2**(1), 1–6.

Burow, K.R., Belitz, K., Dubrovsky, N.M. & Jurgens, B.C. 2017. Large decadal-scale changes in uranium and bicarbonate in groundwater of the irrigated western US. *Science of the Total Environment* **586**, 87–95.

Census (2011), Primary Census Abstracts, Registrar General of India, Ministry of Home Affairs, Government of India, Available at: http://www.censusindia.gov.

Central Ground Water Board (CGWB). (n.d.). Retrieved October 23, 2020, from http://cgwb.gov.in/reportspublished.html

Central Water Commission. 2015. Retrieved June 15, 2020, from http://cwc.gov.in/sites/default/files/annual-report-cwc-2015-16.pdf

Cheremisinoff, P.N., 2019. *Handbook of water and wastewater treatment technology*. Routledge, 840 pp.

Chinnasamy, P. & Agoramoorthy, G. 2015. Groundwater storage and depletion trends in Tamil Nadu State, India. *Water Resources Management* **29**(7), 2139–2152.

Choubisa, S.L. 2001. Endemic fluorosis in southern Rajasthan, India. *Fluoride* **34**(1), 61–70.

FAO 2016. https://www.google.com/url?sa=t&source=web&rct=j&url=http://www.fao.org/3/a-bp793e.pdf&ved=2ahUKEwie3KnVlcvwAhXVjOYKHYWZAQYQFjAEegQIERAC&usg=AOvVaw0Dd_v_Javwix8lUPsgg5Qj

Gaillardet, J., Dupré, B., Louvat, P. & Allegre, C.J. 1999. Global silicate weathering and CO2 consumption rates deduced from the chemistry of large rivers. *Chemical geology* **159**(1–4), 3–30.

Gardner, R.C. & Davidson, N.C. 2011. The ramsar convention. In *Wetlands*, Springer, Dordrecht, pp. 189–203.

Gebrehiwot, A.B., Tadesse, N. & Jigar, E. 2011. Application of water quality index to assess suitablity of groundwater quality for drinking purposes in Hantebet watershed, Tigray, Northern Ethiopia. *ISABB Journal of Food and Agricultural Sciences* **1**(1), 22–30.

Gjessing, E. 1976. Physical and Chemical Characteristics of Aquatic Humus. Ann Arbor Science Publishers, Michigan. https://doi.org/10.4319/lo.1976.21.6.0932

Harikumar, P.S. & Chandran, M. 2013. Bacteriological Contamination of Groundwater Due to Onsite Sanitation Problem in Keraka State: A Case Study. *International Journal of Life Sciences Biotechnology and Pharma Research* **2**(3), 190–202. https://doi.org/10.1155/2019/4307251

IMD Annual Report 2018. Retrieved December 30, 2020, from https://metnet.imd.gov.in/imdnews/ar2018.pdf

IMD Annual Report 2019. Retrieved December 30, 2020, from https://metnet.imd.gov.in/imdnews/ar2019.pdf

Jasmin, I. & Mallikarjuna, P. 2014. Physicochemical quality evaluation of groundwater and development of drinking water quality index for Araniar River Basin, Tamil Nadu, India. *Environmental monitoring and assessment* **186**(2), 935–948.

Jaya Divakaran, S., Sara Philip, J., Chereddy, P., Nori, S.R.C., Jaya Ganesh, A., John, J. & Nelson-Sathi, S. 2019. Insights into the bacterial profiles and resistome structures following the severe 2018 flood in Kerala, South India. *Microorganisms* **7**(10), 474.

Jia, L., Wang, R., Feng, L., Zhou, X., Lv, J. & Wu, H. 2018. Intensified nitrogen removal in intermittently-aerated vertical flow constructed wetlands with agricultural biomass: effect of influent C/N ratios. *Chemical Engineering Journal* **345**, 22–30.

Katz, B. G., Coplen, T.B., Bullen, T.D. & Davis, J.H. 1997. Use of chemical and isotopic tracers to characterize the interactions between ground water and surface water in mantled karst. *Groundwater* **3**5(6), 1014–1028.

Kulkarni, H., Shah, M. & Shankar, P.V. 2015. Shaping the contours of groundwater governance in India. *Journal of Hydrology: Regional Studies* **4**, 172–192.

Mahler, B.J. & Garner, B.D. 2009. Using nitrate to quantify quick flow in a karst aquifer. *Groundwater* **47**(3), 350–360.

Manjula, P. & Warrier, C.U. 2019. Evaluation of water quality of Thuthapuzha Sub-basin of Bharathapuzha, Kerala, India. *Applied water science* **9**(4), 1–13.

Mattson, M.D. 2009. Alkalinity. Encyclopedia of Inland Waters, 1–6. https://doi.org/10.1016/b978-012370626-3.00090-9

Mishra, P.C. & Patel, R.K. 2003. Study of the pollution load in the drinking water of Rairangpur, a small tribal dominated town of North Orissa. *Aquatic Ecosystems* **379**.

Mukherjee, A., Saha, D., Harvey, C.F., Taylor, R.G., Ahmed, K.M. & Bhanja, S.N. 2015. Groundwater systems of the Indian sub-continent. *Journal of Hydrology: Regional Studies* **4**, 1–14.

Nair, A., Joseph, K.A. & Nair, K.S. 2014. Spatio-temporal analysis of rainfall trends over a maritime state (Kerala) of India during the last 100 years. *Atmospheric Environment* **88**, 123–132.

Nair, H.C., Padmalal, D., Joseph, A. & Gopinthan, V.P. 2018. Hydrogeochemistry and water quality assessment of shallow aquifers in the western flanks of Southern Western Ghats, SW India. *Arabian Journal of Geosciences* **11**(4), 1–32.

NITI Aayog 2018. Composite water management index. National Institution for Transforming India, GOI.

Patel, P., Raju, N.J., Reddy, B.S.R., Suresh, U., Gossel, W. & Wycisk, P. 2016. Geochemical processes and multivariate statistical analysis for the assessment of groundwater quality in the Swarnamukhi River basin, Andhra Pradesh, India. *Environmental Earth Sciences* **75**(7), 611.

Piper, A.M. 1944. A graphic procedure in the geochemical interpretation of water-analyses. *Eos, Transactions American Geophysical Union* **25**(6), 914–928.

Prasad, G., Kentilitisca, J.Y., Ramesh, M.V., Suresh, N. 2020. An Overview of Natural Organic Matter. In: Kumar, A., Paprzycki, M., Gunjan, V. (eds) ICDSMLA 2019. Lecture Notes in *Electrical Engineering* **601**, Springer, Singapore.

Prasad, G. & Ramesh, M.V. 2019. Spatio-temporal analysis of land use/land cover changes in an ecologically fragile area—Alappuzha District, Southern Kerala, India. *Natural Resources Research* **28**(1), 31–42.

Prasad, G., Rajesh, R. & Arun, K. 2020. Land Use Pattern as an Indicator of Sustainability: A Case Study. *In 10th Annual International Conference on Industrial Engineering and Operations Management.* IEOM Society International. ISSN, pp. 2169–8767.

Prasad, G., Thomas, G.M. & Ramesh, M.V. 2021. Trace metal analysis of pre-flood and post-flood drinking water at Alappuzha District, Southern Kerala, India. *Materials Today: Proceedings* **46**, 2911–2918.

Raj, D. & Shaji, E. 2016. Fluoride contamination in groundwater resources of Alleppey, southern India, *Geoscience Frontiers*. doi: 10.1016/j.gsf.2016.01.002

Rajapurkar, M.M., John, G.T., Kirpalani, A.L., Abraham, G., Agarwal, S.K., Almeida, A.F., ... & Jha, V. 2012. What do we know about chronic kidney disease in India: first report of the Indian CKD registry. *BMC nephrology* **13**(1), 1–8.

RamyaPriya, R. & Elango, L. 2018. Evaluation of geogenic and anthropogenic impacts on spatio-temporal variation in quality of surface water and groundwater along Cauvery River, India. *Environ Earth Sci*. **77**(2). https://doi.org/10.1007/s12665-017-7176-6

Reza, R. & Singh, G. 2019. Application of heavy metal pollution index for ground water quality assessment in Angul District of Orissa, India. *International Journal of Environmental Sciences* **5**(1).

Rohde, M.M., Froend, R. & Howard, J. 2017. A global synthesis of managing groundwater dependent ecosystems under sustainable groundwater policy. *Groundwater* **55**(3), 293–301.

Schoeller, H. 1977. Geochemistry of groundwater. In 'Groundwater Studies–an International Guide for Research and Practice'. (Eds RH Brown, AA Konoplyantsev, J. Ineson, and VS Kovalevsky) pp. 1–18.

Sivanandan Achari, P.D. & Ambili, M.S. 2018. Groundwater Quality Of Andhakaranazhy Coast, Alappuzha, Kerala, India.

Susheela, A.K. 1991. Prevention and control of Fluorosis: Skeletal fluorosis-symptoms.

Tiwari, T.N. & Mishra, M.A. 1985. A preliminary assignment of water quality index of major Indian rivers. *Indian J. Environ Prot*. **5**(4), 276–279.

Todd, D.K. 1980. *Ground water hydrology*. Wiley, New York, 552 pp.

Varma, A. 2017. *Groundwater resource and governance in Kerala*. Status, issues and prospects. Forum for Policy Dialogue on Water Conflicts in India, 118 pp.

Verma, D.K., Bhunia, G.S., Shit, P.K., Kumar, S., Mandal, J. & Padbhushan, R. 2017. Spatial variability of groundwater quality of Sabour block, Bhagalpur district (Bihar, India). *Applied Water Science***7**(4), 1997–2008.

Vutla, B.M.S. & Ravichandran, S. 2011. Groundwater Quality and Role of the Monsoon in Chennai City, South India. *Asian Journal of Chemistry* **23**(10), 4659.

WHO (2003). Total dissolved solids in drinking water, Background documents for development of WHO guidelines for drinking water quality. World Health Organisation. http://www.who.int/water_sanitation_health/dwq/chemicals/tds.pdf. Accessed May 2020

WHO (2011). Guidelines for Drinking-water Quality, Fourth Edition World Health Organization.

Zhang, Y., Shi, P., Li, F., Wei, A., Song, J. & Ma, J. 2018. Quantification of nitrate sources and fates in rivers in an irrigated agricultural area using environmental isotopes and a Bayesian isotope mixing model. *Chemosphere* **208**, 493–501.

Zucker, I., Mamane, H., Cikurel, H., Jekel, M., Hübner, U. & Avisar, D. 2015. A hybrid process of biofiltration of secondary effluent followed by ozonation and short soil aquifer treatment for water reuse. *Water Research* **84**, 315–322.